

# Calcium-sensing receptor expression in insulin-negative, intrapancreatic insulinoma

Weikun Qian<sup>1,2</sup>, Liang Han<sup>1,2</sup>, Wei Li<sup>1,2</sup>, Wanxing Duan<sup>1,2</sup>, Zhenhua Ma<sup>1,2</sup>, Qingyong Ma<sup>1,2</sup>, Zheng Wu<sup>1,2</sup> and Zheng Wang<sup>1,2,\*</sup>

<sup>1</sup>Department of Hepatobiliary Surgery, The First Affiliated Hospital of Xi'an Jiaotong University, Xi'an, China

<sup>2</sup>Pancreatic Disease Centre of Xi'an Jiaotong University, Xi'an, China

\*Correspondence to: Zheng Wang, Department of Hepatobiliary Surgery, The First Affiliated Hospital of Xi'an Jiaotong University, 277 West Yanta Road, Xi'an 710061, China (e-mail: zheng.wang11@mail.xjtu.edu.cn)

Dear Editor

Pancreatic neuroendocrine tumours (p-NETs) are a group of tumours with neuroendocrine differentiation<sup>1</sup>.

A 66-year-old man who had experienced paroxysmal unconsciousness after fatigue or hunger, accompanied by eye gaze and stiff limbs, for 6 months was referred to the hospital. He first went to the department of neurology; doctors found no abnormalities on cranial imaging, but a 4-cm space-occupying mass in the pancreatic head which was accompanied by obvious dilatation of the pancreatic duct. Enhanced CT showed a non-homogeneous enhancement mass in the head of pancreas (Fig. 1a, red arrow) with two intrapancreatic duct masses on the arterial phase of abdominal enhanced CT (yellow and blue arrows). Levels of carbohydrate antigen (CA)19-9, CA125, and neurone-specific enolase were within the normal range, but the immune-reactive insulin (IRI)/blood glucose ratio was up to 1.24. A typical Whipple's triad was detected at 6:00 hours on the second morning in hospital. The patient declared no previous disease history or long-term medication history.

A diagnosis of insulinoma was suspected and a standard pancreatoduodenectomy was performed. Interestingly, two polypoid bulges were observed in the pancreatic duct besides the pancreatic main mass, but the duct was not invaded by tumour; the tumour was simply growing along the lumen (Fig. 1b). Histopathological examination of these masses revealed a uniform solid, trabecular, and nest structure accompanied by hypervascularity and without nesidioblastosis in adjacent normal pancreas (Fig. 1c). Immunostaining was positive for chromogranin A and synaptophysin, but, strangely, negative for insulin (less than 1 per cent focal insulin-positive tumour cells) (Fig. 1d). Hence, the pathological diagnosis was G2 (5 per cent Ki-67-positive, mitosis 2 per 2 mm<sup>2</sup>) p-NET.

After resection, the paroxysmal hypoglycaemia did not recur. In contrast, transient postoperative rebound hyperglycaemia was observed. Postoperative PET-CT showed no retained mass in the pancreas. The follow-up data revealed that the patient's IRI and C-peptide levels exhibited a stable trend after undergoing a significant decline. Hence, the suggested diagnosis was insulin staining-negative (type IV non-granular), intrapancreatic ductal insulinoma. Indeed, to recognize this

unusual p-NET, screening was undertaken for a possible molecular marker named calcium-sensing receptor (CaSR) according to the GSE73338<sup>2</sup> (Fig. 1e), and strong expression was found, even in insulin-negative insulinoma (Fig. 1f).

Another case of insulin-negative insulinoma has been reported<sup>3</sup>. It may not be accurate to diagnose p-NET solely by staining for hormone indicators because abnormal storage and rhythmic release of insulin are pathophysiological mechanisms of insulinoma<sup>4</sup>. However, staining for CaSR, a critical molecule in the cellular calcium pathway (core signalling of islet cells on releasing insulin), maybe a useful marker for distinguishing pathological subgroups of p-NET, and even for recognizing insulin-negative insulinoma. Doctors should first exclude the diagnosis of non-functional p-NET combined with nesidioblastosis or microinsulinoma and other p-NET-related special syndromes<sup>5</sup>.

## Funding

This work was supported by grants from the National Natural Science Foundation of China (82103117) and the Science and Technology Innovation Team Programme of Shaanxi Province (2022TD-43 and 2022PT-35).

## Acknowledgements

Written informed consent was obtained from the patient for this case report and all the accompanying pictures and data.

## Disclosure

The authors declare no conflict of interest.

## References

1. Ney A, Canciani G, Hsuan JJ, Pereira SP. Modelling pancreatic neuroendocrine cancer: from bench side to clinic. *Cancers (Basel)* 2020;**12**:3170
2. Sadanandam A, Wullschlegel S, Lyssiotis CA, Gröttinger C, Barbi S, Bersani S et al. A cross-species analysis in pancreatic neuroendocrine tumors reveals molecular subtypes with

Received: April 11, 2022. Revised: May 03, 2022. Accepted: May 06, 2022

© The Author(s) 2022. Published by Oxford University Press on behalf of BJS Society Ltd.

This is an Open Access article distributed under the terms of the Creative Commons Attribution-NonCommercial License (<https://creativecommons.org/licenses/by-nc/4.0/>), which permits non-commercial re-use, distribution, and reproduction in any medium, provided the original work is properly cited. For commercial re-use, please contact [journals.permissions@oup.com](mailto:journals.permissions@oup.com)

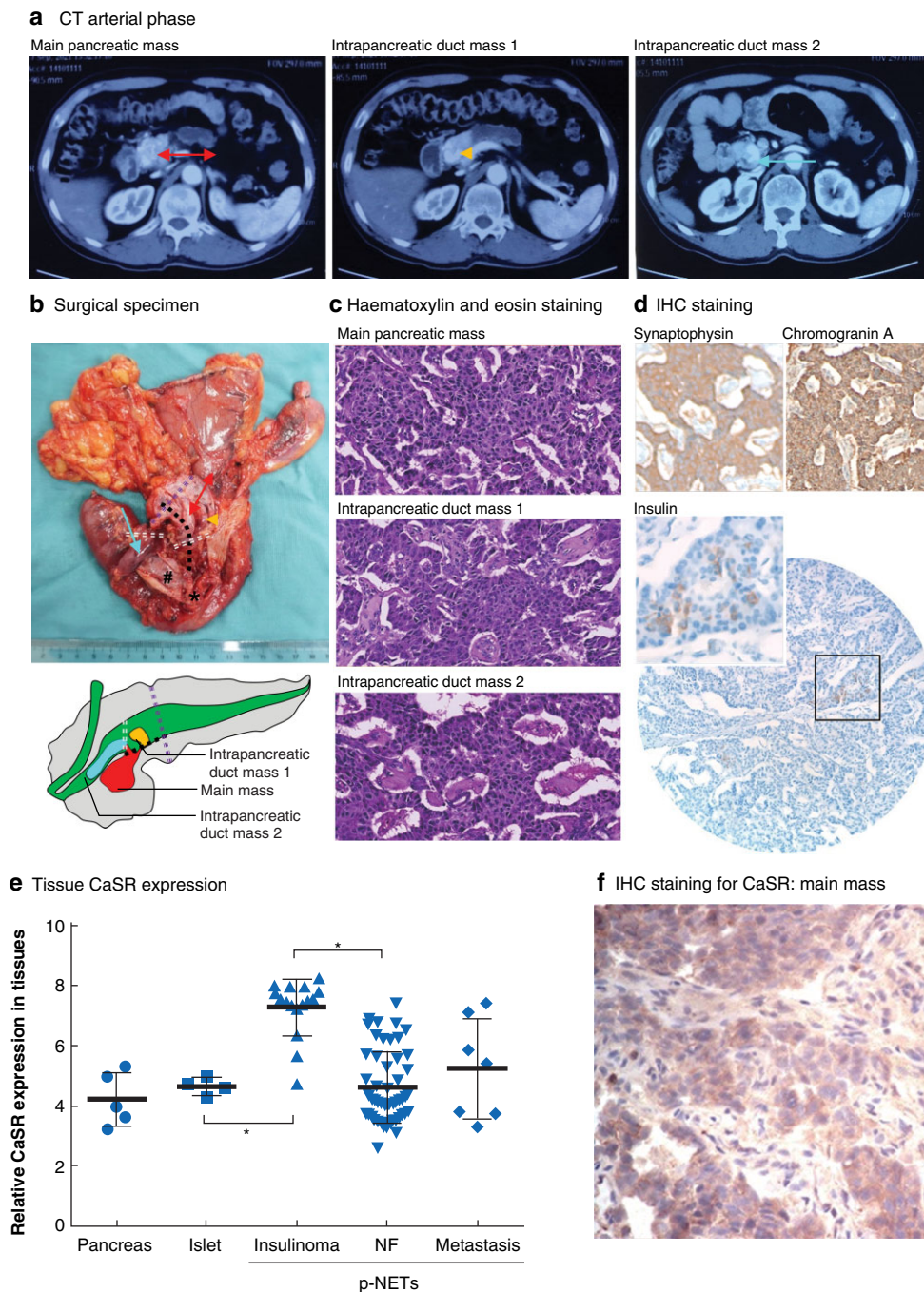


**Fig. 1** Evaluation of patient with insulin-negative, intrapancreatic insulinoma

**a** Three-phase enhanced CT images of patient before hospital admission, showing main pancreatic mass in unciform process (double-head arrow), intrapancreatic duct mass 1 (arrow head), and intrapancreatic duct mass 2 (single-head arrow). **b** Anatomical location in surgical specimen showing main pancreatic mass in unciform process (double-head arrow), intrapancreatic duct mass 1 (arrow head), intrapancreatic duct mass 2 (single-head arrow), dilated pancreatic duct (symbol #), duodenal papilla (symbol \*), surgical margin of pancreatic duct (treble-row dotted line), dissection margin for separating intrapancreatic duct mass (double-row dotted line), and dissection margin for exposing main pancreatic mass in unciform process (single-row dotted line); diagram of pancreas is shown below. **c** Microscopic view of haematoxylin and eosin-stained sections of the three masses (original magnification  $\times 200$ ). **d** Immunohistochemical (IHC) staining for chromogranin A (CgA), synaptophysin (Syn), and insulin in main pancreatic mass in unciform process (original magnification of CgA, Syn and Insulin  $\times 200$  and interested magnification of Insulin  $\times 400$ , hematoxylin counterstain). **e** Relative calcium-sensing receptor (CaSR) expression in normal pancreas, normal islets, insulinoma, non-functional (NF) pancreatic neuroendocrine tumours (p-NETs), and metastatic p-NETs according to GSE73338 data sets. Bold line and error bars represent mean value and standard deviation. \* $P < 0.050$  (Limma-trend test which based on empirical Bayes prior trend embedded in limma package of R software). **f** IHC staining for CaSR in insulin-negative insulinoma tissue (main pancreatic mass in uncinate process) (original magnification  $\times 400$ , hematoxylin counterstain).

distinctive clinical, metastatic, developmental, and metabolic characteristics. *Cancer Discov* 2015;**5**:1296–1313

3. Roth J, Klöppel G, Madsen OD, Storch MJ, Heitz PU. Distribution patterns of proinsulin and insulin in human insulinomas: an immunohistochemical analysis in 76 tumors. *Virchows Arch B Cell Pathol Incl Mol Pathol* 1992;**63**:51–61

4. Nessa A, Rahman SA, Hussain K. Hyperinsulinemic hypoglycemia—the molecular mechanisms. *Front Endocrinol (Lausanne)* 2016;**7**:29

5. van Beek DJ, Nell S, Verkooijen HM, Borel Rinkes I, Valk GD, Vriens MR. Surgery for multiple endocrine neoplasia type 1-related insulinoma: long-term outcomes in a large international cohort. *Br J Surg* 2020;**107**:1489–1499